Adsorption 3, 81–91 (1996)

Adsorbents from Waste Materials

ATTILA BÓTA, KRISZTINA LÁSZLÓ AND LAJOS GYÖRGY NAGY
Department of Physical Chemistry, Technical University Budapest, Hungary, H-1521 Budapest, Hungary
klaszlo@ch.bme.hu

GÜNTER SUBKLEW, HEIDE SCHLIMPER AND MILAN J. SCHWUGER
Institute of Applied Physical Chemistry, Research Center Jülich, Germany D-52425 Jülich, Germany

Abstract. The possibility of using pyrolyzed wastes produced in already working incineration plants, as adsorbents for waste water treatment, was studied. Showing very poor adsorption properties, they were improved by steam activation technique used in the conventional activated carbon manufacturing. It is concluded that various organic waste materials can be converted to carbonaceous final products with a character similar to activated carbon. Their adsorption properties and pore size distribution are determined by the structure of the starting material. Although most of these samples have a low specific surface area, their pore volume is not negligible in the meso- and micropore range. Adsorption tests with model waste waters confirmed that adsorption properties are strongly influenced by the character of the surface. The adsorption capacity of these samples can be utilized for the treatment of strongly polluted industrial waste waters. Considering that the raw material 'needed' to manufacture these adsorbents is produced permanently and the adsorbents do not have to be regenerated, it might be worthwhile using these kinds of adsorbents in the primary treatment of industrial waste waters.

Keywords: activated carbon, solid organic waste

1. Introduction

Activated carbon is an adsorbent most often used in waste water treatment. Commercially available activated carbons are tailor made for this application. Raw materials are carefully selected and transformed by an optimized process to an adsorbent, having the desired mechanical strength, particle size, specific surface area, pore size, pore size distribution, etc. These carbons have a high and constant quality making their price relatively high as well. Their starting materials are fossil coals or organic materials rich in carbon, e.g., polymers or different parts of plants. Throughout the world agricultural by-products, such as by-products of the timber industry (e.g., sawdust) or different agricultural by-products, such as straw, rice hull, seeds or fruit stones are some of the raw materials used in active carbon production (László et al., 1995; Rodriguez-Reinoso and Molina-Sabio, 1992; Gergova et al., 1994; Lussier et al., 1994; González et al., 1994; Benke, 1993; Bóta et al., 1992; Noszkó et al., 1984; Rivera-Utrilla et al., 1991).

Development of waste management policies is an urgent issue all over the world. More and more waste is produced by human beings. Landfilling sites are becoming full and—as people are more and more concerned about their environment—hard to find, not mentioning the increasing costs. There is a huge amount of solid wastes, containing a relatively high percentage of organics, which can be and already are reasonably reduced by volume in incinerators. The usage of these carbon-containing wastes in primary waste water treatment can be a two-fold solution to environmental problems. It reduces the volume of the wastes and an increasing demand for water treatment might be fulfilled at a reasonable price. Another advantage in application of these adsorbents is that there is no need to regenerate them because of their low production costs.

However, carbon-containing industrial and household wastes have not been considered favourable raw materials for the production of activated carbon because their composition can be variable and inhomogeneous, furthermore, their carbon content can be very low. Part of the difficulties can be overcome by selective collection and processing of the wastes. Thermal processing of these wastes is carried out by pyrolysis at 500–700 °C with the exclusion of oxygen. In this process, as in the first step of the active carbon production, the organic part of the waste gets partly carbonized. The result is that the carbonized (pyrolyzed) product bears features characteristic to the starting material (Bóta et al., 1993).

In the present work different selectively collected wastes pyrolyzed in incineration plants were studied in their original form and after steam activation in order to determine their capability in waste water treatment. For comparison, a commercial activated carbon produced especially for waste water treatment was studied.

2. Experimental

Starting Materials

A relatively wide variety of selectively collected and pyrolyzed wastes was used in the experiments. Therefore, their quality based on carbon content was very different as well. Domestic waste (DOW) was mostly made of perishable garbage produced by households. Car industry produces a huge amount of "carbon rich" wastes, and from there we investigated autoshredder light fraction (ASL) and tire rubber (GUM). The light fraction of the autoshredder contains all the inner soft parts of the car remaining after the removal of metallic parts. An other waste product of the automobile industry is tires. Tires have a high carbon content since soot is used as filler in tire manufacturing. Pyrolyzed steelless tire were used as sample. Packaging materials are produced and consumed on a large scale. Pyrolyzed paper (PPR) and poly-ethyleneterephthalate (PTF) were used from this group of wastes. The symbols given in parentheses are used to identify the pyrolyzed samples obtained by the pyrolysis of the wastes in incineration plants in Germany.

Activation

In order to improve adsorption capacity, the pyrolyzed substances were subjected to activation. Before the activation step, all samples were heated at 700 °C for 30 min, since the thermal record of the different samples were rather diverse. Each sample was subjected to a briquetting process because the pyrolyzed samples were in pulverized form with a very wide size distribution. Briquetting was performed by adding 20 wt% bitumen dissolved in xylene to the dried sample. The mixture obtained was dried and pressed (ca 40 kN/m^2) into flat sheets with a thickness of about 3 mm. The addition of bitumen increased the carbon content of the samples by 4 to 5%. Platelets were crushed and samples with a grain size of about 3 to 5 mm were activated in a steam flow of 18 g/h at 900 °C in a rotary quartz reactor (Noszkó et al., 1984). The steam was diluted with nitrogen in a molar ratio of 1 : 1. The weight loss due to activation (the extent of burn-off) was determined.

Characterization of the Samples

Raw materials were pyrolyzed up to 1000 °C in nitrogen. The weight loss was assigned to the amount of volatile components removed in the carbonization process. The ash content was determined similarly by measuring the weight of the solid residue after incinerating the sample in air.

After activation the samples were characterized based on the adsorption capacity for iodine and methylene blue, the specific surface area, the pore volume and the pore size distribution. The 'true' and the apparent densities were also measured. The 'true' density of the solid matrix was determined by the helium pycnometer method. The apparent density was calculated from the volume of the pycnometer closely packed with the powdered sample and from the sample weight.

Iodine and methylene blue adsorption was determined according to NORIT. These kinds of measurements are generally applied as fast industrial test methods for controlling the quality of the adsorbents. Iodine number informs about the internal surface of the activated carbon. 1 mg of iodine (molecular area: 0.15–0.42 nm^2) adsorbed is considered to represent 1 m^2 internal surface. Methylene blue (molecular area: 0.54–1.97 nm^2) value reveals the adsorptive properties of a carbon towards larger organic molecules.

Nitrogen adsorption/desorption isotherms were used to determine the specific surface area, the specific pore volume and the pore size distribution of the

samples in the mesopore range. The isotherms were measured at the boiling point of liquid nitrogen by AUTOSORB-1 (Quantachrome, Syosset, NY, USA) computer controlled automatic surface analyser and data processing system. Specific surface area was calculated according to the multi-point B.E.T. method. The total pore volume was derived from the amount of vapour adsorbed at a relative pressure close to unity, assuming, that the pores are filled with liquid nitrogen. The pore size distribution was computed using the method proposed by Barrett et al. (1951). The t-method of Halsey (1948) was used for the determination of micropore volume in the presence of mesopores.

The matrix structure of the samples was studied by small angle X-ray scattering (SAXS) technique. Ground samples with an average particle size of 10 μm were placed into 1-mm thick sample holder and covered by Mylar foil. The scattering of Ni filtered Cu K_α-radiation ($\lambda = 0.1542$ nm) was recorded in the $1 \cdot 10^{-2}$–1 nm^{-1} range of scattering variable, defined as $s = 2(\sin\theta)/\lambda$, where 2θ and λ are the scattering angle and the wavelength, respectively. A classical Kratky camera and a proportional counter (Anton Paar, Graz, Austria) were used. Data were evaluated by the method based on the moments of the scattering intensity function (Jánosi and Stoeckli, 1979).

Adsorption Tests

As we would like to apply these activated 'carbons' for waste water treatment, samples were tested with model synthetic waste waters. Typical organic compounds representing a variety of different pollutants were used in diluted aqueous solutions. One of the important features of the activated carbons used in waste water treatment is their capability to adsorb phenol, for phenol is one of the most frequent contaminants in industrial waste waters (Magne and Walker, 1986; Urano et al., 1982). Besides being carcinogenic, a very uncomfortable feature of phenol is that, it reacts with the chlorine producing carcinogenic chlorinated compounds (Ferro-Garcia et al., 1993; Rivera-Utrilla et al., 1991; Worch et al., 1990), which was represented by 2,3,4-trichlorophenol in our experiments. The family of the polyaromatic hydrocarbons was represented by naphthalene, while from among herbicides atrazine (2-chloro-4-ethylamino-6-isopropylamino-1,3,5-triazine) was used.

The performance of our carbons was compared to that of a commercial activated carbon produced especially for waste water treatment, i.e., F200 (Calgon Carbon Corp. Pittsburg, PA, USA). Equilibrium adsorption isotherms were determined in static batch experiments at ambient temperature (László et al., 1993). The solutions were not buffered, the pH was found to be 7.5 to 8.9. Stoppered flasks were shaken in a thermostat shaker to reach equilibrium. The solid/liquid ratio was changed systematically in order to get the adsorption isotherms from the low equilibrium concentration up to the saturation value. Starting concentration of the solutions was limited by the low solubility of the solutes. Saturated solutions were used except phenol, which was used in a stock solution of 500 mg/l. Contact times were concluded from preliminary kinetic experiments. Samples were shaken for 24 hrs. with phenol solution, 72 hrs. with trichlorophenol, 5 days with atrazine and 6 days with naphthalene. Starting and equilibrium concentrations were determined by detecting the UV absorption of the phenols ($\lambda = 254$ nm) and atrazine ($\lambda = 220$ nm) using a Merck-Hitachi 655A UV HPLC monitor and a UVIKON 930 UV/visible spectrofotometer (Kontron, Zurich, Switzerland), respectively. To obtain a better accuracy, naphthalene was determined with an LS fluorescence spectrometer (Perkin-Elmer, Ueberlingen, Germany) at $\lambda = 254$ nm. Measured data were evaluated according to the Langmuir model.

3. Results and Discussion

Characterization of the Starting Material

Pyrolyzed autoshredder light fraction, tire rubber, domestic waste and different packing materials were chosen to be tested. The homogenized and dried wastes pyrolyzed in incineration plant were characterized by their composition. Data in Table 1 were obtained from thermoanalytical measurements performed up to 1000°C. According to the volatile matter values the thermal record of the samples were very diverse. The ash content was found to be considerably high. According to X-ray fluorescence analysis it mainly consists of silicates insoluble in water. The pyrolyzed carbonaceous substances were also characterized considering some of their surface properties (Table 2). Both the specific surface area and the pore volume of the pyrolyzed samples are small values. It can be explained either with the compactness of the structure or/and the

Table 1. Composition of the pyrolyzed materials[1].

Pyrolyzed substances from	Symbol	Ash content[2] wt%	Volatile matter[3] wt%	Carbon content[4] wt%
Domestic waste	DOW	57	31	12
Auto tire	GUM	19	10	71
Shredder light fraction	ASL	65	25	10
Poly-ethyleneterephtalate	PTF	1	1	98
Packing paper	PPR	20	19	61

[1]Data were determined from thermogravimetric measurements. About 0.1 g of homogenized powdered samples (A) were heated up to 1000 C at a rate of 10 C/min. The measurement was performed both in air and nitrogen and final weight was determined as B in air and C in nitrogen, respectively.
[2](B/A) · 100.
[3]((A-C)/A) · 100.
[4]((C-B)/A) · 100.

Table 2. Surface characterization of the pyrolyzed samples.

Pyrolyzed substance	a_s, N_2, BET m^2/g	Pore volume[1] cm^3/g	Average pore radius[2] nm
Domestic waste	34	0.086	5.02
Auto tire	20	0.18	18.6
Shredder light fraction	15	0.044	5.87
Polyethyleneterephthalate	12	0.010	1.56
Packing paper	649	0.59	1.81

[1]The volume of the pores was obtained from the adsorption isotherms as the volume of liquid nitrogen filling up the pores at a relative pressure of about 1.
[2]Obtained as $r_p = \frac{2V_{liq}}{a_{s,N_2,BET}}$, where V_{liq} is the volume of the adsorbed nitrogen, assuming cylindrical pore geometry.

mostly closed pores. The only exception is the PPR sample, where the porous structure starts developing simultaneously with the carbonization.

Improvement of the Adsorption Behaviours

In order to increase the low specific surface areas and thus the adsorption capacities of the pyrolyzed substances, the samples were activated. It must be underlined, that in this case the task was not to produce an optimal activated carbon for a given purpose but to utilize all possibilities involved in a hardly optimal raw material. Nevertheless PTF and PPR may provide an ideal starting material for activated carbon, having high carbon and low ash contents, although their structure

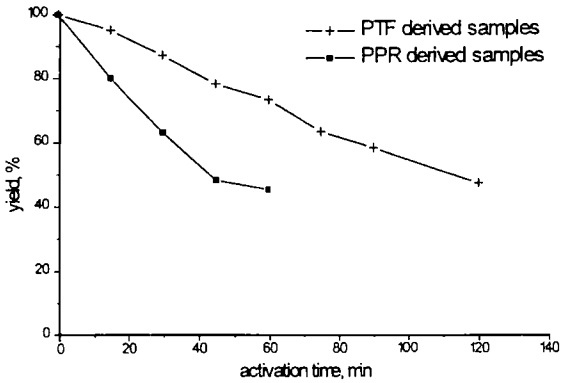

Figure 1. The progress of the activation in time.

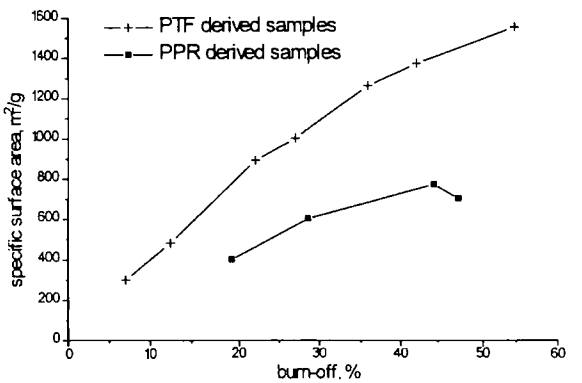

Figure 2. Development of the specific surface area during the activation. Specific surface area was calculated from iodine adsorption (NORIT).

is different according to the different structure of the starting plastic and the cellulose. Therefore, these two samples were used to illustrate that the character of the activated product is affected by both the starting raw material and the duration of the activation process.

The progress of the activation may be followed by the yield, i.e., the extent of "burn-off". Figure 1 shows that the same activation time results in a different yield, depending on the raw material. This difference can be even better illustrated by the development of the inner surface area or the pore volume during the activation (Fig. 2). According to its high specific surface area, the carbon obtained from PTF can be considered as a microporous system beyond burn-off of ca. 30%. It is also proven by the methylene blue uptake (Fig. 3). The methylene blue adsorption up to a burn-off value of 30% is independent from the origin of the sample, although the corresponding specific surface area value (Fig. 2) of the PTF-originated sample is significantly

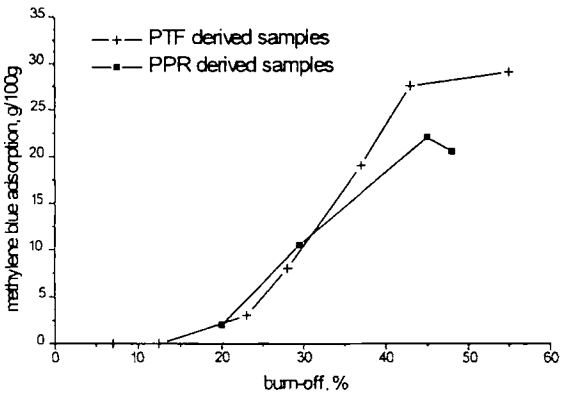

Figure 3. Change of the methylene blue value (NORIT) during the activation.

higher than that of the PPR-carbon in this burn-off range.

Characterization of the Activated Samples

The pyrolyzed samples were all activated for 30 min. Yields are given in Table 3. The weight loss occurring during the activation process corresponds to the partial burn-off of the carbon content and the removal of the colloidal-size inorganic particles carried away from the samples by the nitrogen - steam mixture passing through the reactor during the activation treatment. Therefore, the yield is not directly related to the carbon gasified. That is the reason that the DOW and PPR derived samples had about the same yield in spite of their different carbon content or that the DOW and ASL samples (both having ca 10 wt% carbon content) produced different yield after 30 min activation. Nevertheless, the too high carbon burn-off results in an enrichment of the non-volatile inorganic part and therefore decreases also the relative amount of the carbon in the product. It may be noted that the GUM derived sample has a relatively high yield considering its carbon content. The reason probably is that its carbon content is mainly present in the form of chemically resistant carbon black particles.

The specific surface areas calculated from the nitrogen adsorption data according to the BET model and the iodine and methylene blue numbers listed in Table 3 indicate that very different adsorbents were obtained from the different raw materials. There is no correlation between the burn-off values and specific surface areas. The inorganic components present in most of the wastes might have a modifying effect on the surface properties of the activated adsorbents.

The pore structure and the chemical character of an adsorbent is reflected in the interaction with the adsorbed nitrogen molecules. The well-known Dubinin-Radushkevich equation (Dubinin, 1975) derived on the basis of the volume-filling theory of micropores was applied to fit the low-pressure region of the nitrogen adsorption isotherms shown in Fig. 4. The parameters of the D-R equation were determined and the characteristic adsorption energies (E_a) were calculated. These values giving the differential molar heat of adsorption at an adsorbed amount equal with the $1/e$ fraction of the saturation capacity were found to change from 6.4 to 8.5 kJ/mol. The higher values were obtained in the cases of the PTF and PPR derived sample, which can be attributed to the microporous character of these carbons.

The pore structure of the activated samples were characterized on the basis of the low-temperature nitrogen adsorption/desorption isotherms in the

Table 3. Characterization of the activated samples.

Sample derived from	Yield %	I_2-number mg/g $\Delta \pm 3\%$	a_s, N_2, BET m^2/g $\Delta \pm 5\%$	Methylene blue number g/100 g $\Delta \pm 5\%$	Pore volume[1] cm^3/g $\Delta \pm 5\%$	Average pore radius[2] nm $\Delta \pm 12\%$
DOW	65	105	87	2.3	0.16	3.80
GUM	82	170	142	2.0	0.29	4.15
ASL	70	280	221	6.0	0.21	1.94
PTF	89	540	693	0	0.38	1.11
PPR	62	680	577	16.1	0.42	1.46

[1]The volume of the pores was obtained from the adsorption isotherms as the volume of liquid nitrogen filling up the pores at a relative pressure of about 1.

[2]Obtained as $r_p = \frac{2V_{liq}}{a_{s,N_2,BET}}$, where V_{liq} is the volume of the adsorbed nitrogen, assuming cylindrical pore geometry.

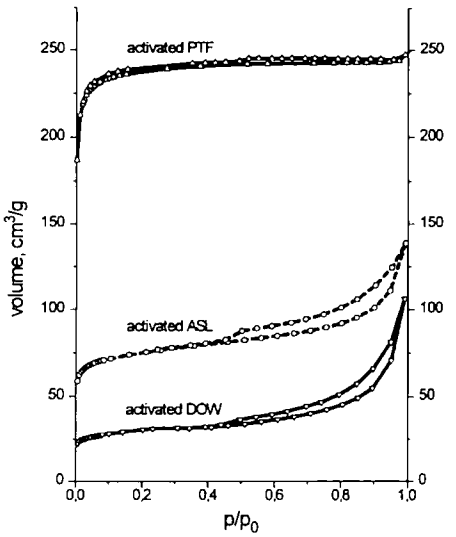

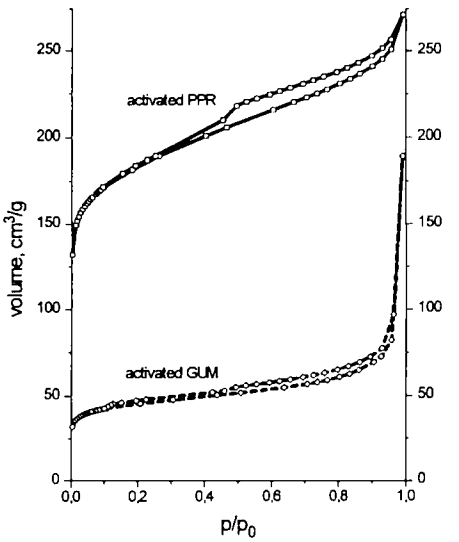

Figure 4. Low temperature (77 K) adsorption/desorption isotherms of the 30-min activated samples.

micro- and mesopore range. The pore volume of the micropores in the DOW, ASL and GUM derived samples is small when compared to that of the PTF and PPR samples since micropores can develop mainly from the reactive carbonaceous part of the raw material. A significant pore volume can be assigned in the mesopore range (Table 4) even for samples having relatively low specific surface area.

The adsorption isotherms in Fig. 4 were converted into *t*-plots (Fig. 5). The adsorbed amount is plotted against the average thickness of the adsorbate layer

Table 4. Pore size volume of the activated samples.

Activated sample from	Volume of the micropores[1] cm^3/g	Volume of the mesopores[2] cm^3/g	Total volume of the pores[3] cm^3/g
DOW	0.040	0.105	0.16
GUM	0.067	0.210	0.29
ASL	0.093	0.076	0.21
PTF	0.360	0.010	0.38
PPR	0.265	0.069	0.42

[1]Determined by the B-point method (Gregg and Sing, 1967) from the isotherms in Fig. 4.

[2]The volume of the pores in the pore size range of 4 < Radius, nm < 100 obtained from the adsorption isotherms as the volume of liquid state N_2 filling up the pores in the $0.65 < p/p_0 < 0.99$ range of relative pressure.

[3]The volume of liquid state N_2 filling up the pores at ca 0.99 relative pressure.

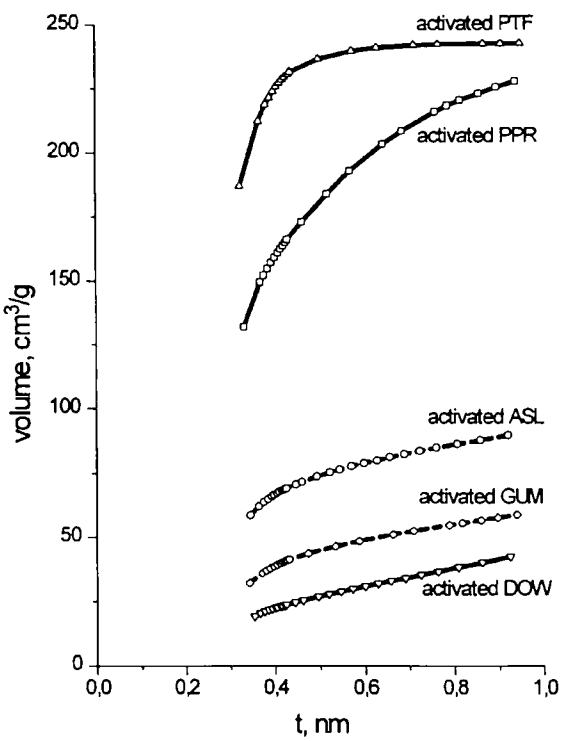

Figure 5. *t*-plot of the 30-min activated samples, calculated by the Halsey-equation.

on a flat surface having an identical surface character as the adsorbent in question. It should be understood that for non-porous material the *t*-plot is a straight line starting from the origin with a slope equal to the

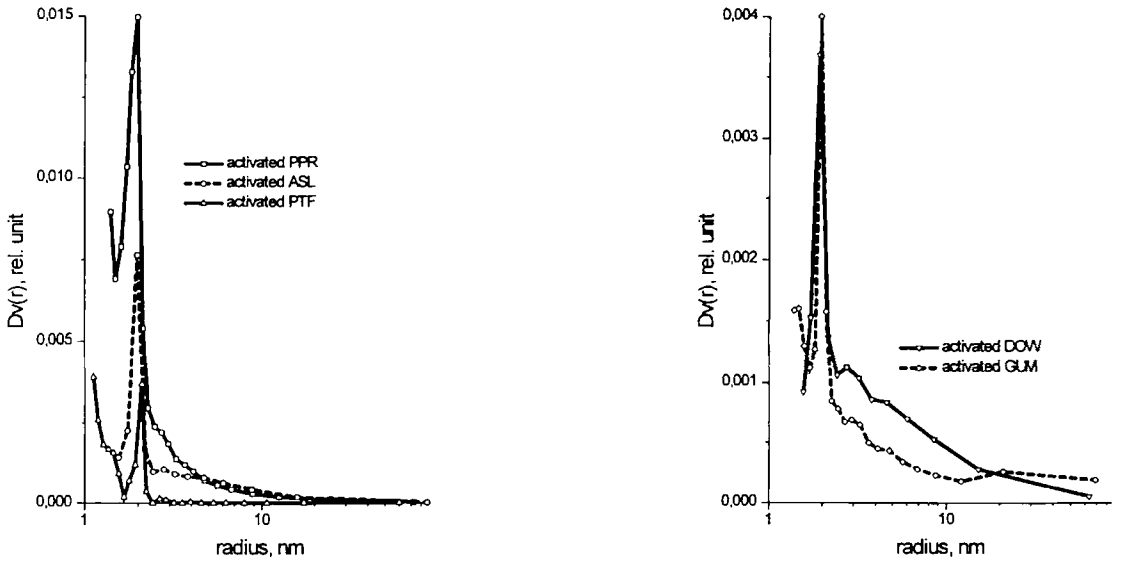

Figure 6. Pore size distribution of the 30-min activated samples in the mesopore range calculated from the isotherms in Fig. 4.

specific surface area, for a porous material the slope decreases as some of the pores are filled up and the surface available for adsorption 'disappears'. Upward deviation from the straight line indicates the occurrence of capillary condensation in the pores. The t-functions in this paper were calculated by the Halsey-equation. There is only a slight deviation from the linear in the case of activated DOW samples. In the ASL, GUM and PPR derived samples pores with all sizes are about equally represented, however, the total micropore volume is small in the case of ASL and GUM derived samples since micropores can develop mainly from the relative carbon containing components present originally in relatively small amount in the raw materials of these samples (Fig. 5). The activated PTF sample shows a sharp bend characteristic to microporous systems. On the curves representing the distribution of the mesopore volume by pore size a sharp peak appears at about $r_p \approx 2$ nm for all the samples (Fig. 6). A second peak can be observed on the curve of the GUM derived sample between 20–30 nm. This later peak may reflect the size of the carbon black crystallites used in the tire manufacturing.

The small angle X-ray scattering (SAXS) gives further details about the fine structure of the samples. From the SAXS curves, the Guinier radius is the most frequently obtained parameter. On replotting the scattering data according to the Guinier approximation, no linear log $I(s)$ vs. s^2 plots were obtained. That means, that the size-distribution of the scattering units is heterodisperse and a single Guinier radius can not be assigned to these systems. In order to determine characteristic particle sizes from the SAXS measurements the method of moment was applied. The calculated parameters were the reduced chord length (l_r) and the correlation distance (l_c). The reduced chord length represents the average length of all segments drawn across the matrix in all directions, which is defined by the following equation:

$$l_r = \int_0^\infty sI(s)\,ds/2\pi \lim_{s\to\infty} s^3 I(s)$$

where $I(s)$ is the measured, with line-focus smeared intensity. The correlation distance corresponds to the average crystallite size obtained from the wide-angle X-ray scattering data, defined by:

$$l_c = \int_0^\infty I(s)\,ds.$$

The latter quantity is very sensitive to the corrections relating to multiple scattering in the range of the very small s values. Therefore the accuracy of the determination of this 0th moment is estimated to be approximately 20%.

The porous material was considered a two-phase system comprising solid matter and voids (pores). From

Table 5. Change of the structure during the activation.

Sample		l_c nm $\Delta \pm 10\%$	l_r nm $\Delta \pm 3\%$	l_m^1 nm $\Delta \pm 10\%$	l_p^1 nm $\Delta \pm 10\%$
DOW	Pyrolyzed	9.3	3.1	4.6	9.7
	activated	6.6	4.5	6.6	14.0
GUM	Pyrolyzed	6.0	1.9	2.8	5.8
	activated	5.9	3.0	4.2	10.3
ASL	Pyrolyzed	7.1	4.0	6.0	12.1
	activated	4.2	1.6	2.3	5.5
PTF	Pyrolyzed	2.8	0.35	1.5	0.46
	activated	2.6	0.41	0.7	1.0
PPR	Pyrolyzed	10.5	1.2	2.8	2.1
	activated	6.6	1.0	1.3	4.7

[1] $l_m = l_r/P$, and $l_p = l_r/(1-P)$, where P is the volume fraction of the pores in the sample, and calculated as $P = 1 - \rho/\rho_{He}$, where ρ and ρ_{He} are the bulk and the true densities, resp.

Table 6. Specific surfaces of the samples determined by SAXS method.

Sample		$f = l_c/2l_r$	$S_{\text{sheet like}}$ m^2/g	$S_{\text{cylindrical}}$ m^2/g
DOW	Pyrolyzed	1.5	139	—
	activated	0.7	—	287
GUM	Pyrolyzed	1.6	345	—
	activated	1.0	232	580
ASL	Pyrolyzed	0.9	—	339
	activated	1.3	345	864
PTF	Pyrolyzed	3.6	690	—
	activated	3.2	1450	—
PPR	Pyrolyzed	4.4	310	—
	activated	3.2	650	—

At $f > 1$ sheet like units and at $f \sim 1$ cylindrical units with equal diameter and height were supposed.

the reduced chord length the average lengths in the solid and the pores, l_m and l_p, respectively, were calculated (Glatter and Kratky, 1991). SAXS data are calculated in Table 5. The size of the coherent region (l_c) decreases during the activation, indicating the increasing inhomogeneity within the structure. The variation in the mean wall thickness (l_m) is different. It increases in the DOW and GUM samples, therefore it can be supposed that the smaller units are less resistant during the activation because of their amorphous structure, thus the activation in these cases results in the enrichment of the larger units in the remaining solid matrix at this conversion. The wall thickness seems to increasing in the DOW sample which is rich in inorganic particles of colloidal size. Similar effect is caused in activated GUM samples by the resistency of the carbon black particles. In the further cases a more than 50% decrease in the l_m values occur. In the ASL derived sample a thermal fission of the inorganic particles may occur. In the carbon rich PTF and PPR derived samples the effect can be attributed to the chemical reaction between the steam and the carbon skeleton containing mostly amorphous carbon besides the graphite-like units.

The specific surface area can be calculated from the SAXS data if we suppose a concrete pore geometry. To find the proper pore geometry a form factor (f) can be easily derived from the calculated SAXS parameters, $f = l_c/2l_r$. $f > 1$, when the scattering units form a lamellar structure, while $f < 1$ when the units have close to uniform geometry. The form factors and the specific surface areas are summarized in Table 6. Generally, the SAXS surfaces of the pyrolyzed samples show higher values than the BET surfaces, because the samples in their pyrolyzed form contain closed pores unavailable for the adsorbing gas molecules. Surprisingly this is not the case with the PPR sample. In this sample the forming of the pores, probably run parallel with the pyrolysis. In the activated samples the specific surface areas are significantly higher than the BET surfaces, showing that the inner surface has not be opened up totally by activation.

Adsorption Test with Synthetic Waste Waters

Some data characterizing the synthetic pollutant molecules are collected in Table 7. Molecular areas are given supposing flat conformation of the adsorbed molecules. Naphthalene is a completely nonpolar molecule, while phenol is the most polar one among the remaining three compounds. The amount of each pollutant adsorbed by 1 g of carbon was calculated by $m_a = \frac{V \cdot \Delta c}{m}$, where V is the volume of the synthetic waste water, m is the mass of the carbon and Δc is the difference of the initial and equilibrium concentrations in the liquid phase. The commercial F200 was used as standard. Its specific surface area (nitrogen, BET) was 692 m^2/g, the total pore volume 0.43 cm^3/g and the average pore radius was found to be 0.98 nm.

Adsorption isotherms in all cases when they could be measured were of type of L according to Gile's classification. Carbons giving an isotherm of L-type

Table 7. Physico-chemical properties of the pollutant molecules.

Pollutant	Molar mass	Solubility 20°C	Molecular area nm^2/molecule
Phenol	94.11	82 g/l (Roth, 1991)	0.522 (Magne and Walker, 1986) 0.544 (Snyder, 1968)
2,3,4-trichlorophenol	197.45	ca. 0.4 g/l	0.72 (Snyder, 1968)
Naphthalene	128.9	ca. 20 mg/l (0.155 mmol/l)	0.82 (Snyder, 1968)
Atrazine	215.7	30–70 mg/l (Rippen) (0.139–0.325 mmol/l)	0.90 (Snyder, 1968)

are considered to have an excess of acidic surface groups (Rudling and Björkholm, 1986). L-type isotherms level out at higher sample concentration, corresponding to completion of a monolayer in the experimental concentration range. Although the conditions of the Langmuir model are not fulfilled in the case of these carbons, isotherms were relatively well fitted (R = 0.92–0.99) by the linear Langmuir-equation which was used to determine the adsorption capacity.

As it could be expected from the specific surface area and pore volume values, the equilibrium of phenol and trichlorophenol uptake of the pyrolyzed samples proved to be very poor, except PPR and PTF, i.e., the samples with high reactive carbon content. No correlation was found between the nitrogen specific surface area or pore volume and the adsorption capacity values (László et al., 1995). The phenol adsorption of the pyrolyzed domestic waste was almost negligible (Hakim, 1992). The pyrolyzed tire sample did not adsorb phenol at all, due to its hydrophobic surface character, arising from the carbon black. There is also a significant difference between the phenol and trichlorophenol uptake in the case of the ASL sample (about 50% on molar base). The pollutant uptake of the pyrolyzed samples was found to be only a few % of the standard's, therefore they can not be suggested as reasonable adsorbents in waste water treatment (László et al., 1993).

As it was demonstrated previously in this paper, the activation process considerably improved the nitrogen adsorption capacities and the pore structure. The activation process results in higher specific surface area and therefore a significantly better pollutant uptake, as it is illustrated in the case of the adsorption of phenol on pyrolyzed and activated autoshredder (Fig. 7). At the same time it has to be mentioned that steam activation

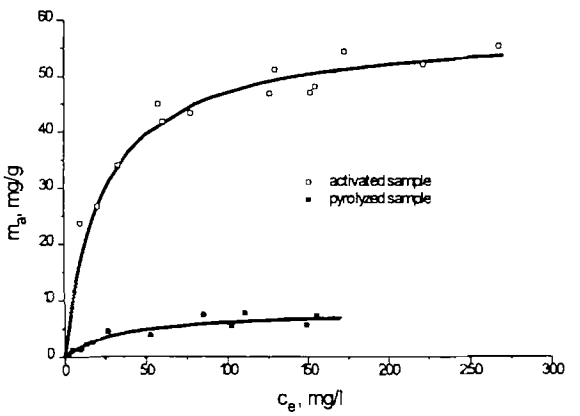

Figure 7. Adsorption of phenol on ASL derived samples at ambient temperature.

has affected the polarity of the surface as well, e.g., tire sample adsorb both phenol and trichlorophenol after the activation.

The results of the adsorption tests performed with synthetic model waste waters on activated samples are expressed both in grams and moles in Table 8. Among the activated PTF and PPR derived samples the ones with the highest specific surface area were investigated. Activation times of these samples were 90 min and 45 min, and the specific surface areas (N_2, BET) were 1103 m^2/g and 606 m^2/g, respectively. The pore volume and the average pore radius were 0.63 cm^3/g and 0.9 nm, respectively, in the case of PTF-derived sample and 0.50 cm^3/g and 1.4 nm, respectively, in the case of PPR-derived sample. Comparing the saturation adsorption capacity values, it shows that the activated adsorbents derived from raw materials with high non-resistant carbon and low ash content have uptake values that compare favorably with the commercial activated carbon.

Table 8. Adsorption capacities of the activated samples[1].

	Sample	Phenol	2,3,4-trichloro-phenol	Naphthalene	Atrazine	a_s, N_2, BET m^2/g
DOW	m_m mg/g	21.62	—	—	—	87
	n_m mmol/g	0.2297	—	—	—	
	G μmol/m^2	2.64	—	—	—	
GUM	m_m mg/g	43.24	78.0	—	—	142
	n_m mmol/g	0.4595	0.3950	—	—	
	G μmol/m^2	3.23	2.9	—	—	
ASL	m_m mg/g	57.34	110.0	—	—	221
	n_m mmol/g	0.6093	0.5571	—	—	
	G μmol/m^2	2.76	2.7	—	—	
PTF[2]	m_m mg/g	286.70	764.36	595.20	449.28	1103
	n_m mmol/g	3.046	3.8711	4.6431	2.0829	
	G μmol/m^2	2.76	3.5	4.2	1.9	
PPR[2]	m_m mg/g	109.04	399.91	249.60	434.16	606
	n_m mmol/g	1.1586	2.0254	1.9471	2.028	
	G μmol/m^2	1.91	3.3	3.2	3.3	
F200	m_m mg/g	140.06	498.41	492.80	267.84	692
	n_m mmol/g	1.4882	2.5242	3.8443	1.247	
	G μmol/m^2	2.15	3.6	5.6	1.8	

[1]Monolayer capacities were calculated from the linear Langmuir plot: $\frac{c_e}{m_a} = \frac{1}{K \cdot m_m} + \frac{1}{m_m} c_e$, where c_e is the concentration of the liquid phase in the equilibrium state, m_m is the adsorption capacity and K is constant.
[2]PTF and PPR derived samples with the highest specific surface area were tested (activation time was 90 min and 45 min, respectively).
[3]G values were calculated from the mmol/g data and the BET specific surface area values.

4. Conclusion

The carbonaceous products derived from various organic waste materials demonstrated an activated-carbon-like character. The adsorption properties and pore size distributions of these products were determined by the structure of the starting materials. Although most of these samples had a relatively low specific surface area, their pore volume was not negligible in the meso- and micropore range. Their adsorption capacity could be utilized in the treatment of strongly polluted industrial waste waters. Adsorption tests with one-solute model waste waters confirmed that the adsorption properties were influenced by the surface character.

Domestic waste could not be reasonably used even in activated form, but the activated tire and autoshredder derived samples performed about one third of the standard's phenol capacity. The adsorption capacity of the samples derived from raw materials rich in chemically non-resistant carbon, such as PPR or PTF, compared favorably with commercial activated carbon. Considering that the raw materials 'needed' to manufacture these adsorbents are produced permanently and the adsorbents do not have to be regenerated, it might be worthwhile to use these kinds of adsorbents in the treatment of industrial waste waters.

Nomenclature

a_s, N_2, BET	Specific surface area calculated from gas adsorption data according to BET model	m^2/g
c_e	Equilibrium concentration	m mol/l
E_a	Adsorption energy from D-R-plot	kJ/mol
K	Constant	l/mol
I	Small angle scattering intensity of X-ray	
l_c	Correlation distance	nm
l_m	Length in the solid mater	nm
l_p	Length in the pores	nm
l_r	Reduced chord length	nm
m	Mass of the carbon	g
m_a	Mass of pollutant adsorbed by 1g of adsorbent at a given equilibrium concentration	mg/g

m_m	Adsorption capacity	mg/g
n_m	Adsorption capacity	mmol/g
P	Volume fraction of the pores	
R	Guinier radius	nm
r_p	Average pore size	nm
s	$(2 \sin \Theta)/\lambda$	
S_p	Specific surface area from X-ray measurements	m^2/g
t	Statistical thickness of the adsorbate layer	nm
V	Volume of synthetic waste water	ml
V_{liq}	Volume of adsorbed nitrogen	cm^3
λ	Wavelength	nm
ρ	Apparent density	cm^3/g
ρ_{He}	Bulk density	cm^3/g
2θ	Scattering angle	
Δc	Difference of the initial and equilibrium concentrations in the liquid phase	g/l
Γ	Adsorption capacity	$\mu mol/m^2$

Acknowledgment

The authors wish to express their appreciation for the financial support provided by the OTKA Fund (Budapest, Hungary), Project No. T 017019, Ms. Emese Fülöp and Mr. György Bosznai for their experimental work.

References

Barrett, E.P., L.G. Joyner, and P.P. Halenda, "Determination of Pore Volume and Area Distributions in Porous Substances. I. Computation from Nitrogen Isotherms," *J. Am. Chem. Soc.*, **73**, 373–380 (1951).

Benke, D., Ph.D. Thesis, University of New South Wales, Adelaide, Australia, 1993.

Bóta, A., K. László et al., "Active Carbon from Waste Materials," in *Proc. of 6th Hungarian Conf. on Colloid Chemistry in Memoriam G. Schay*, Balatonszéplak, p. 173, 1992.

Bóta, A., K. László et al., Aktívszén elöállítása hulladékokból, Magyar Kémiai Folyóirat, **99**(7–8), 316–323 (1993).

Dubinin, M.M., in *Progress in Surface Membrane Science*, D.A. Cadenhead, J.F. Danelli, and M.D. Rosenberg (Eds.), Vol. 9, p. 1, Academic Press, New York, 1975.

El Hakim, Ph.D. Thesis, KFA Jülich, 1992.

Ferro-Garcia, M.A., E. Ultera-Hidalgo, J. Rivera-Utrilla, and C. Moreno-Castilla, "Regeneration of Activated Carbons Exhausted with Chlorophenols," *Carbon*, **31**(6), 857 (1993).

Gergova, K., N. Petrov, and S. Eser, "Adsorption Properties and Microstructure of Activated Carbons Produced from Agricultural By-Products by Steam Pyrolysis," *Carbon*, **32**, 693–702 (1994).

Glatter, O. and O. Kratky (Eds.), *Small Angle X-Ray Scattering*, Academic Press, London, 1982.

González, M.T., M. Molina-Sabio, and F. Rodriguez-Reneiso, "Steam Activation of Olive Stone Chars, Development of Porosity," *Carbon*, **32** 1407–1413 (1994).

Gregg, S.J. and K.S.W. Sing, *Adsorption, Surface Area, Porosity*, Academic Press, London, 1967.

Halsey, G.D., "Physical Adsorption on Nonuniform Surface," *J. Chem. Phys.*, **16**, 931–937 (1948).

Jánosi, A. and H.F. Stoeckli, "Comparative Study of Gas Adsorption and Small Angle X-Ray Scattering by Active Carbons," in *Relation to Heterogeneity, Carbon*, **17**, 465–469 (1979).

László, K., A. Bóta, A. Simay, and L.Gy. Nagy, Hulladékból elöállitott aktívszenek minösítése, Magyar Kémiai Folyóirat, **99**(7–8), 324–327 (1993).

László, K., A. Bóta, A. Simay, L.G. Nagy et al., "Application of Activated Carbon from Waste Materials in Waste Water Treatment," in *Proc. of Challenges and Innovations in the Management of Hazardous Waste Sites*, Washington, D.C., 1995 (in press).

Lussier, M.G., J.C. Shull, and D.J. Miller, "Activated Carbon from Cherry Stones," *Carbon*, **32**, 1493–1498 (1994).

Magne, P. and P.L. Walker, Jr., "Phenol Adsorption on Activated Carbons: Application to the Regeneration of Activated Carbons Polluted with Phenol," *Carbon*, **24**(2), 101–107 (1986).

NORIT Testing Methods, Norit N.V., Holland, Special publication.

Noszkó, L.H., A. Bóta, Á. Simay, and L.Gy. Nagy, "Preparation of Activated Carbon from the By-Products of Agricultural Industry," *Periodica Polytechnica*, **28**, 293–297 (1984).

Rippen—Handbuch Umweltchemikalien—16, *Erg. Lfg.* 7/92, 1–15.

Rivera-Utrilla, J., E. Ultera-Hidalgo, M.A. Ferro-Garcia, and C. Moreno-Castilla, "Comparison of Activated Carbons Prepared from Agricultural Raw Materials and Spanish Lignites When Removing Chlorophenols from Aqueous Solutions," *Carbon*, **29**(4/5), 613–619 (1991).

Rodriguez-Reinoso, F. and M. Molina-Sabio, "Activated Carbons from Lignocellulosic Materials by Chemical and/or Physical Activation: An Overview," *Carbon*, **30**, 1111–1118 (1992).

Roth, Wassergefahrende Stoffe, Vol. 3, 1991.

Rudling, J. and E. Björkholm, "Effect of Adsorbed Water on Solvent Desorption of Organic Vapors Collected on Activated Carbon," *Am. Ind. Hyg. Assoc. J.*, **47**, 615–620 (1986).

Snyder, L.R., *Principes of Adsorption Chromatography*, Marcel Dekker, New York, 1968.

Urano, K., Y. Koichi, and E. Yamamoto, "Equilibria for Adsorption of Organic Compounds on Activated Carbons in Aqueous Solutions," *J. Coll. Interface Sci.*, **86**(1), 43–50 (1982).

Worch, E., R. Kümmel, and R. Büttner, "Zur Anwendung der Potentialtheorie auf die Gemischadsorption Aus waßeringen Lösungen," *Chem. Techn.*, **42**(9), 399–402 (1990).